

STUDY OF THE PRESSING OPERATION OF LARGE-SIZED TILES USING X-RAY ABSORPTION

(1) J.L. Amorós, (1) G. Mallol, (1) D. Llorens, (1) J. Boix, (1) J.M. Arnau, (1) C.Feliu, (2) J.A. Cerisuelo, (2) J.J. Gargallo

(1) Instituto de Tecnología Cerámica (ITC).
 Asociación de Investigación de las Industrias Cerámicas (AICE).
 Universitat Jaume I. Castellón. Spain
 (2) Zirconio, S.A. Villarreal, Castellón. Spain

ABSTRACT

An apparatus has been designed, built, and patented that is able, non-destructively, to determine bulk density distribution in large-sized ceramic tiles. The proposed measurement method, based on the X-ray absorption technique, provides numerous advantages compared with the methods used to date: it enables complete maps of the bulk density distribution in the tiles to be obtained, and is neither destructive nor toxic. The measurements are performed with a low-power X-ray emitter tube. The measurement system is housed in a shielded enclosure.

This technique has been used to examine ceramic tiles fabricated under different industrial conditions, modifying press operating parameters. The use of high-precision laser telemeters also enables maps of tile thicknesses to be obtained, which allows tile mass distribution to be determined. The combination of these three variables: bulk density, thickness, and mass, makes it much easier to interpret the manufacturing defects that may originate in the forming and/or firing stage.



1. INTRODUCTION

1.1. Bulk density measurement methods

The porosity of the ceramic body decisively affects green tile behaviour during processing (drying, glazing, and firing) and largely determines end-product properties (dimensions, curvature, frost resistance, mechanical strength, presence of black core, surface finish, etc.). This makes thorough control essential of the porosity of freshly pressed compacts, in order to assure appropriate further processing and to keep end-product properties within pre-set variation margins [1]. In industrial practice, given the difficulty involved in directly measuring ceramic tile porosity, the physical magnitude that is actually controlled is the bulk density of the unfired body.

Historically, unfired tile bulk density has been determined by the mercury displacement method. The main advantages of this destructive technique lie in its ease of use and high precision (absolute error of ± 4 kg/m³ [2]). It is a destructive, discontinuous, and manual method, however, while the high toxicity of mercury also entails important health risks for the operators that perform such industrial compaction controls. These disadvantages have led to the search and development of new methods for the determination of bulk density in ceramic tiles in recent years [3]. The first improvements consisted of the determination of sample volume from the upthrust undergone by the test pieces when they were submerged in water. Though the precision of the resulting bulk density measurement was acceptable, this new method was not widely accepted on an industrial level because it was more laborious and remained destructive, discontinuous, and manual.

A series of devices then appeared that allowed the bulk density to be measured of samples cut from a tile, based on the determination of their apparent volume by a method other than that of immersion in a liquid. These methods notably included, on the one hand, the reconstruction of sample volume using laser telemeters and, on the other, a method based on the measurement of the volume of water displaced by the sample, which was protected by a plastic membrane, when it was introduced into a mass of water. Despite the good measurement precision provided by some of these devices, the method used remained destructive and discrete.

The Instituto de Tecnología Cerámica (ITC) has recently published a series of research papers [4][5] on two prototypes for the determination of ceramic tile bulk density, using methods based on the measurement of a property directly related to bulk density. These non-destructive methods are the non-contact ultrasound method and the X-ray absorption method. Unlike all previous methods, these methods are non-destructive and allow maps to be obtained of bulk density distribution in entire tiles. The good results obtained in these studies have led to the development and construction of an apparatus for the non-destructive measurement, by X-ray absorption, of bulk density distribution in industrial ceramic tiles [6]. The present study describes the most important technical characteristics of the apparatus,



together with a series of experiments that demonstrate the system's capabilities in studying ceramic tile forming conditions.

1.2. Measurement of bulk density by X-ray absorption.

The measurement of bulk density by X-ray absorption is based on the Lambert-Beer law of absorption, according to which, when electromagnetic radiation crosses a given material, the fraction of incident radiation that is absorbed by the material depends exclusively on the material's chemical nature, thickness, and bulk density [7]. Equation 1 represents the Lambert-Beer law applied to monochromatic radiation and to a perfectly homogeneous material in all its thickness:

$$\frac{I}{I} = e^{-\mu h \rho}$$

Equation 1.

where $I_{\scriptscriptstyle 0}$ is incident radiation intensity, I is transmitted radiation intensity, h is the thickness of the material, ρ is bulk density, and μ is the mass absorption coefficient for the radiation wavelength.

If the nature of the material is not modified and the thickness is known, it is thus possible to determine the material's bulk density from the quantity of absorbed energy. In practice, however, equation 1 is only approximate because the X-ray tubes customarily used for this type of test emit polychromatic radiation and the analysed materials are usually not homogeneous. This significantly complicates the relationships between transmitted radiation intensity and the X-ray absorption coefficient, which depends on incident radiation wavelength [8]. If it were assumed that the analysis region is sufficiently small to be considered homogeneous, the bulk density measurement would not be limited by the heterogeneities in the material. In contrast, the dependence of the absorption coefficient on incident radiation energy makes the analytical resolution of equation 1 quite difficult in order to calculate the density of the material. For this reason, in practice, the simplest approach is to obtain the absorption coefficient of the material to be analysed by prior calibration.

Figure 1 schematically illustrates the developed bulk density measurement system. The piece to be examined (1) is set vertically in a metal frame (figure 2) with a travelling metal plate fitted with a telemetry system (2) that measures the thickness of the piece, an X-ray emitter tube (3), and a radiation sensor (4). In testing, the measurement system performs successive scans from right to left, at a maximum rate of 1000 mm/s, with a minimum vertical displacement between the horizontal lines of 1 mm. As the device travels across the tile, it takes measurements of tile thickness and the intensity of the radiation that crosses it, with a sampling rate of 10 data per millimetre.



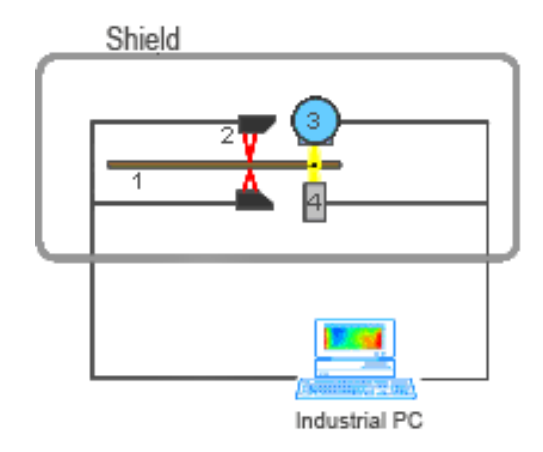


Figure 1. Schematic illustration of the bulk density measurement system by X-ray absorption.

The entire movement and measurement system is closed in a lead shield that prevents any radiation leaks from the X-ray tube. The signals from the different measurement sensors and from the travelling system are fed into a PC with specially developed software for this application, which manages system movements, data processing, and graphic representation.



Figure 2. Internal frame and general view of the bulk density measurement assembly.

The fitted X-ray tube has 50 W power and the radiation sensor used is a ceramic scintillator-photodiode detector. The assembly has been designed to enable unfired industrial tiles with a maximum nominal size of $120~\rm cm~x~60~cm$ and thickness up to $20~\rm mm$ to be tested. When the test is performed at a rate of $500~\rm mm/s$, with a spacing between vertical lines of $5~\rm mm$, the analysis of a tile measuring $120~\rm cm~x~60~cm$ takes about $10~\rm minutes$.

2. METHODOLOGY AND MATERIALS

The measurement of bulk density by X-ray absorption requires previous calibration to establish the relationship between the bulk density of the material being analysed and the attenuation experienced by the radiation. The developed software has a subroutine that allows calibrations to be performed from a series of



test pieces of the same material as that to be analysed. The calibration procedure is usually carried out with cylindrical test pieces, set in a metal holder (see figure 3) for analysis: the mean value of test piece thickness and the intensity of the radiation transmitted through each test piece are then obtained. Using these data and the bulk densities of each test piece determined by a standard method, the software fits the experimental data to equation 1, which yields the characteristic I_0 (V) and μ (m²/kg) values of the studied material.

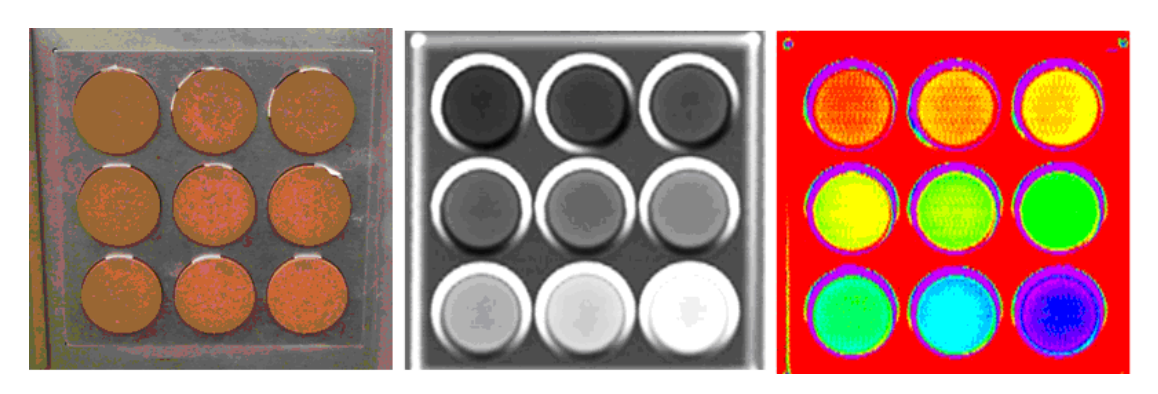


Figure 3. From left to right: calibration test piece holder, test piece X-ray, and bulk density map.

The software application has the capacity to save multiple calibrations in order to test materials of different nature. The performance of a test consists, basically, of placing the piece to be analysed inside the apparatus and, once the shield has closed, to select the corresponding calibration and start the test with given X-ray tube conditions and scanning rate.

The thickness, X-ray intensity, and calculated bulk density values can be visualised while the test is being conducted. The tests can be performed simultaneously on several pieces, which are placed parallel, provided that the total size of the set does not exceed the maximum boundary of the device's inspection area.

The bulk density measurement experiments performed in this study were conducted with two spray-dried powder compositions customarily used for the manufacture of ceramic stoneware floor tiles and porcelain tiles. The test pieces prepared in the laboratory were formed in a hydraulic press equipped with a cylindrical die, 3 cm in diameter, or a $10 \text{ cm} \times 10 \text{ cm}$ square die, depending on experiment needs. The work done on an industrial level was performed in an industrial hydraulic press for the production of porcelain tiles of different sizes.

3. EXPERIMENTAL RESULTS

3.1. Evaluation of measurement method precision.

In order to evaluate the precision of the density measurement method by X-ray absorption, five red stoneware test pieces were prepared, measuring 10 cm \times 10 cm, by pressing at five different maximum pressures. These were then



dried to constant weight in a laboratory oven at 110°C. After the bulk density of the test pieces had been obtained by mercury displacement, their bulk density distributions were determined using a previously conducted calibration. This test was repeated ten times with a view to evaluating the repeatability of the measurement method.

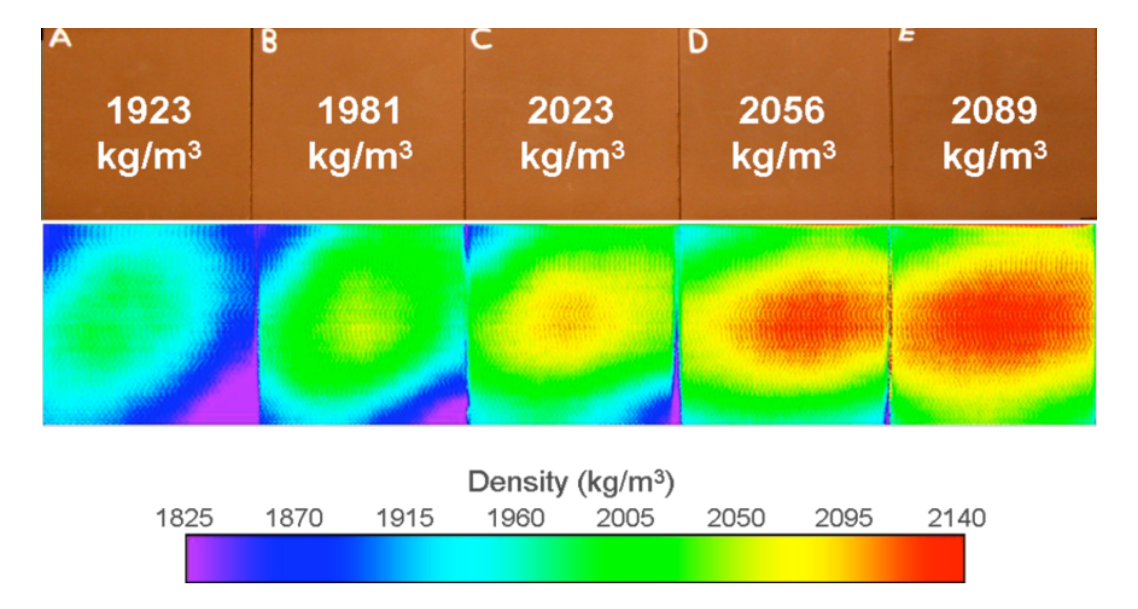


Figure 4. Test pieces used to evaluate the precision of the X-ray absorption method (top) and bulk density distribution maps (bottom).

The top part of figure 4 shows the five analysed test pieces, while the bottom part shows the bulk density distribution maps obtained after the first test. The bulk density values measured by the mercury displacement method and the density values estimated by X-ray absorption in each test are presented in table 1. The agreement between both methods is observed to be very good, the maximum error (difference between the X-ray absorption measurement and the mercury displacement measurement) being 6 kg/m³ and the mean absolute error being 2 kg/m³.

| Ref. | Bulk density by mercury displacement (kg/m³) | Bulk density by X-ray absorption (kg/m³) | | | | | | | | | | |
|------|---|--|------|------|------|------|------|------|------|------|------|---------|
| | | 1 | 2 | 3 | 4 | 5 | 6 | 7 | 8 | 9 | 10 | Average |
| А | 1923 | 1920 | 1923 | 1923 | 1924 | 1923 | 1925 | 1924 | 1922 | 1920 | 1924 | 1923 |
| В | 1981 | 1978 | 1979 | 1979 | 1981 | 1981 | 1982 | 1982 | 1982 | 1982 | 1983 | 1981 |
| С | 2023 | 2020 | 2021 | 2021 | 2025 | 2024 | 2026 | 2026 | 2026 | 2026 | 2026 | 2024 |
| D | 2056 | 2056 | 2058 | 2055 | 2059 | 2059 | 2061 | 2061 | 2061 | 2061 | 2062 | 2059 |
| E | 2089 | 2083 | 2085 | 2083 | 2086 | 2086 | 2087 | 2086 | 2087 | 2087 | 2088 | 2086 |

Table 1. Average bulk densities obtained in the repeatability tests performed with red stoneware test pieces measuring $10 \text{ cm} \times 10 \text{ cm}$.



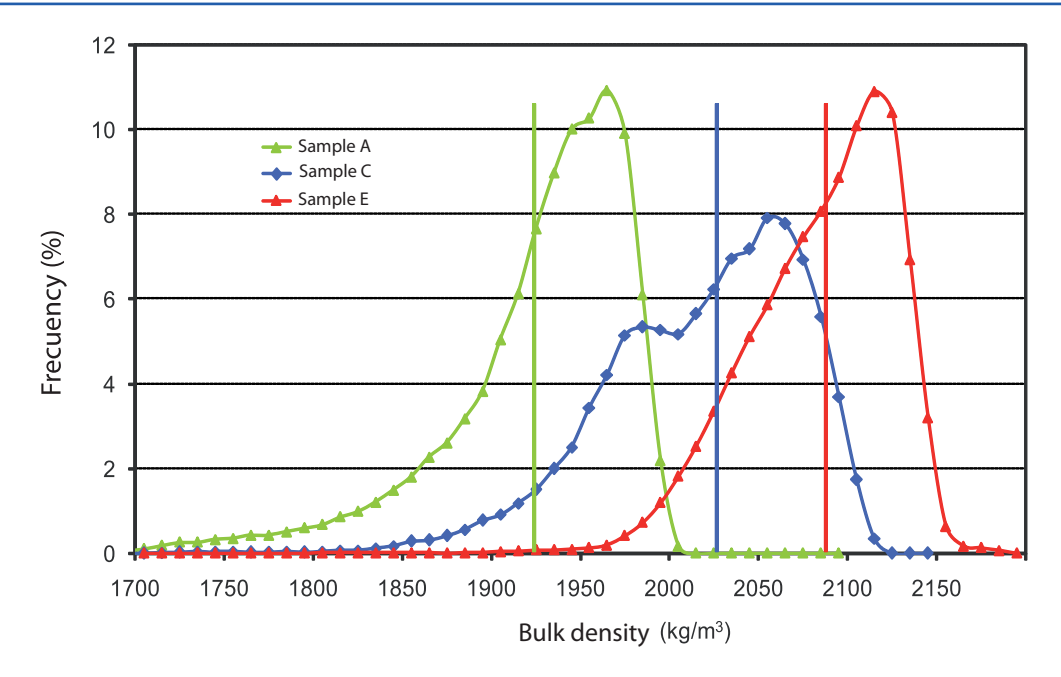


Figure 5. Histograms of the bulk density distributions in pieces A, C, and E obtained by X-ray absorption.

It is interesting to note that the density measurement method by X-ray absorption not only displays the required precision, but it also provides more information than other current methods. In effect, the bulk density distributions map of the test pieces, depicted in figure 4, shows that each piece contains a very heterogeneous bulk density distribution, which is not revealed by the mercury measurement.

By way of example, the histograms of the bulk density distributions measured by X-ray absorption, corresponding to test pieces A, C, and E, together with the values of the average bulk density obtained by mercury displacement (solid vertical lines), are shown in figure 5. It can be observed that, in the case of piece C, the X-ray absorption method provides information on a variation in bulk density of approximately 260 kg/m³, whereas the mercury displacement method only indicates that the average bulk density value of the piece is 2023 kg/m³.

3.2. Use of the X-ray absorption technique for the study of the ceramic tile pressing operation.

3.2.1. Detection of differences in charge, thickness, and bulk density in ceramic tiles.

With a view to evaluating the usefulness of the apparatus for studying the ceramic tile pressing operation, several profiled industrial tiles with a nominal size of 33 cm x 33 cm, obtained under different pressing conditions, were analysed. For this purpose, a series of actions were carried out in an industrial press equipped with a conventional penetrating die with four outputs, fitted with isostatic top punches intended to offset possible charge deficiencies in the cavities.



| Action | Maximum pressure (kgf/cm²) | Charge distribution | | | |
|--------|-------------------------------|---------------------|--|--|--|
| 1 | 335 | Conventional | | | |
| 2 | 285 | Conventional | | | |
| 3 | 335 | Back | | | |
| 4 | 335 | Front | | | |

Table 2. Actions modifying maximum pressing pressure and spray-dried powder charge in an industrial press.

The conditions under which the actions were performed, which basically consisted of the modification of the maximum pressure in the pressing cycle and/ or spray-dried powder charge distribution in the press die cavities, are presented in table 2.

3.2.1.1. Determination of the charge distribution.

Figure 6 shows the surface mass (product ph) distributions corresponding to the four tiles obtained in each action, together with the average values of the surface mass (indicated under the distribution maps) of each tile, the bottom part of the images corresponding to the front of the die. These representations provide information on the charge distribution in the press die cavities when the maximum pressing pressure is applied.

As it may be observed, both the surface mass distribution and the average surface mass values of each tile, in the first two actions, are very similar since the only difference between them is the maximum pressing pressure attained, the spray-dried powder having been charged under the same conditions. Note that, in both actions, the tile corresponding to plate 4 displays an appreciably lower mass than that of the other tiles. Similarly, independently of the position in which the tiles have been pressed, they are all observed to exhibit a slightly displaced charge towards the front of the cavity.

Analysis of the mass distributions corresponding to the tiles in action 3 reveals a considerable increase in the mass introduced into the cavities and a displacement of the charge towards the back of the die, with relation to the values obtained in actions 1 and 2. This change in mass distribution was achieved by cancelling the correction in the position of the bottom punches, which was made in actions 1 and 2 when the powder charging system drew back. That correction enabled a certain quantity of the powder, which had been previously deposited during charge system advance, to be removed from the back of the cavities.

Finally, the mass distribution resulting from action 4 shows that the spraydried powder charge was completely displaced towards the front of the die as a result of an excessive correction of the position of the bottom punches during the retreating movement of the charge system. It may be observed that the average powder mass introduced into each cavity, unlike what occurred in action 3, decreases considerably with respect to actions 1 and 2.



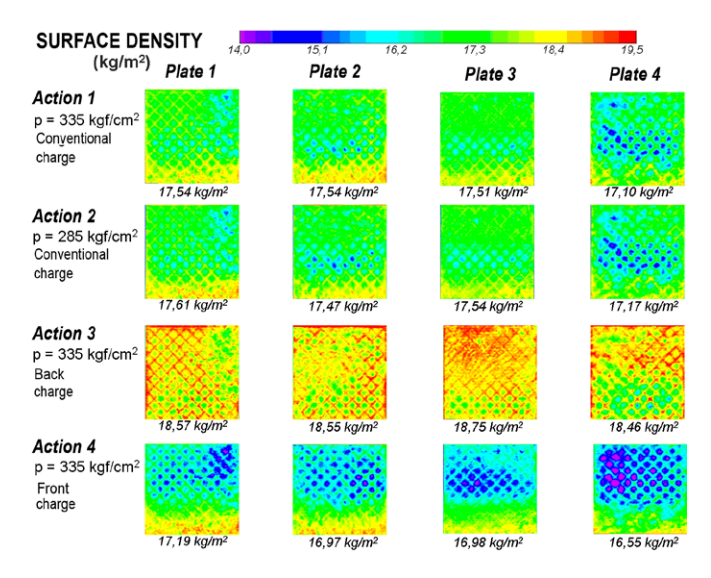


Figure 6. Surface density distributions in the tiles obtained under different pressing conditions.

It may be noted that in all the above actions, the tile pressed in position 4 always displayed a smaller average surface mass. It may similarly be observed that, in the tiles pressed in cavities 1 and 4, there are regions with a low surface mass that remain so, to a greater or lesser extent, throughout all the actions (back right in the tiles from cavity 1 and back left in the tiles from cavity 4). This is related to the profiled tile fair face and highlights the importance of controlling tile design in order to assure good charge distribution.

3.2.1.2. Determination of the thickness distribution.

The thickness distributions obtained in the different actions are shown in figure 7. Comparison of these thickness maps with the mass distributions depicted in figure 6 shows that both variables are closely related. The regions of the tiles with the largest quantity of material are those that are thickest when the pressing cycle ends. Examination of the thickness distributions resulting from actions 1 and 2 shows that these only differ in the average thickness values obtained. The tiles from action 1 are slightly thinner than those from action 2 (the average difference being 0,08 mm), owing to the lower applied maximum pressing pressure. Indeed, at the same quantity of spray-dried powder in the cavities (see figure 6) and at a constant press crosspiece travelling rate, the action 2 pressing cycle reaches the set pressure values earlier and, therefore, provides the tiles with a slightly greater average thickness. With regard to the tiles obtained in action 3, these display a considerably greater average thickness than that of the tiles obtained in actions 1 and 2, as a result of the larger quantity of material in the cavities when the charging cycle ends. In contrast, the lesser thicknesses of the tiles in action 4 are related to the smaller quantity of powder charged in the cavities.

As in the charge distribution, it is interesting to note that, independently of maximum pressing cycle pressure, the thickness distributions of actions 1 and 2 are practically identical. This highlights the great robustness of the spray-dried powder charging systems used in today's industrial presses.



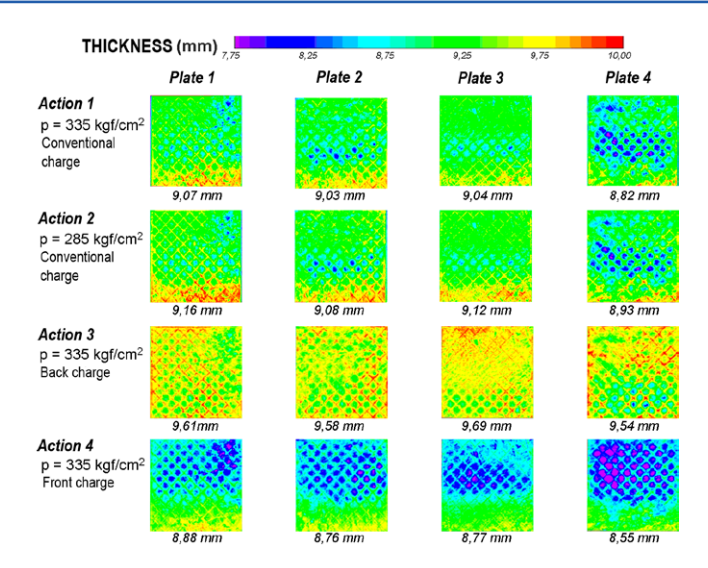


Figure 7. Thickness distributions in tiles obtained under different pressing conditions.

The foregoing indicates that, though there may be shortcomings in the charge distribution in the press cavities, owing to inappropriate regulation of the charging system, these charge differences are not random, but remain constant with time. Such robust behaviour ensures that the adjustments made in the spray-dried powder charging process are immediately reflected in the freshly pressed bodies, and are held throughout the production, provided the nature of the press powder does not change.

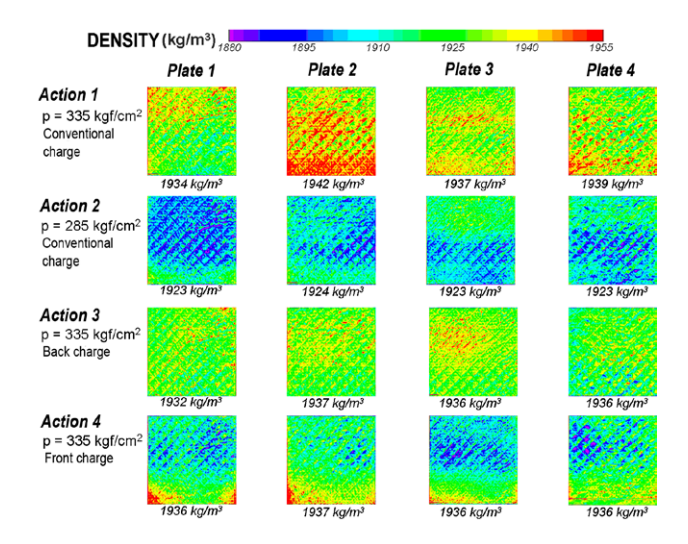


Figure 8. Dry bulk density distributions in tiles obtained under different pressing conditions.

However, owing to their destructive and manual character, the methods used in pressing control on an industrial level do not allow the freshly pressed bodies to be inspected in sufficient detail. As a result, the manufacturing defects related to inappropriate powder distribution in the press cavities are still widely found at present. In this sense, the extent to which measurement by the X-ray absorption method allows complete maps to be obtained of the distribution of three essential variables for pressing control (mass, thickness, and bulk density), makes this method a very useful tool for addressing the manufacturing problems associated with inappropriate pressing operations.



3.2.1.3. Determination of the bulk density distribution.

Finally, figure 8 presents the bulk density distributions of the studied tiles. It may be observed that the average bulk density of the resulting tiles depends exclusively on maximum pressing pressure. In contrast, the density distributions are directly related to the powder distribution in the cavity. On the one hand, the bulk density of the tiles obtained in action 1 is very similar to that obtained in actions 3 and 4, since the maximum applied pressure was 335 kg/cm2 in the three cases. However, the tiles corresponding to action 2 display a lower average bulk density, since they were pressed at 285 kg/cm2. On the other hand, it may be observed that, when the charge is shifted in the cavity (actions 3 and 4), the bulk density distribution changes analogously.

The results of these actions show that detailed analysis of the bulk density distributions by X-ray absorption would allow it to be established if a given tile was liable to exhibit manufacturing defects relating to inappropriate powder distribution in the press die cavity.

3.2.2. Identification of pressing defects in large-sized ceramic tiles.

Figure 9 shows the thickness and bulk density distributions of two smooth porcelain tiles with a nominal size of 45 cm \times 67 cm, obtained in an industrial press fitted with a die with a double matrix, with isostatic bottom punches. The tile pressed in cavity 1 exhibited a homogeneous bulk density distribution; in contrast, the tile pressed in cavity 2 displayed a heterogeneous bulk density distribution, owing to inappropriate operation of the isostatic punch, which led to wedging defects in the end product.

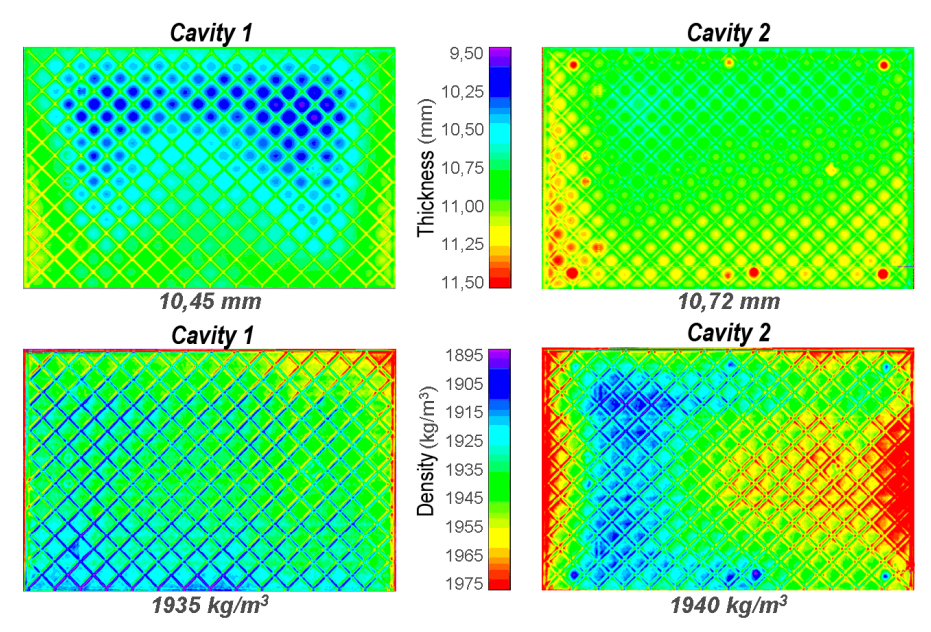


Figure 9. Thickness distributions (top) and dry bulk density distributions (bottom) of two unfired porcelain tiles.

The interpretation of the wedging defect can be completed with the information provided by the thickness distributions of both tiles. It may be observed that tile 1 displays very pronounced differences in thickness, related to the compensation



of pressures applied by the isostatic punch on the powder bed. The effect of the isostatic punch led to a density distribution with average maximum differences in the tile of less than 20 kg/m³.

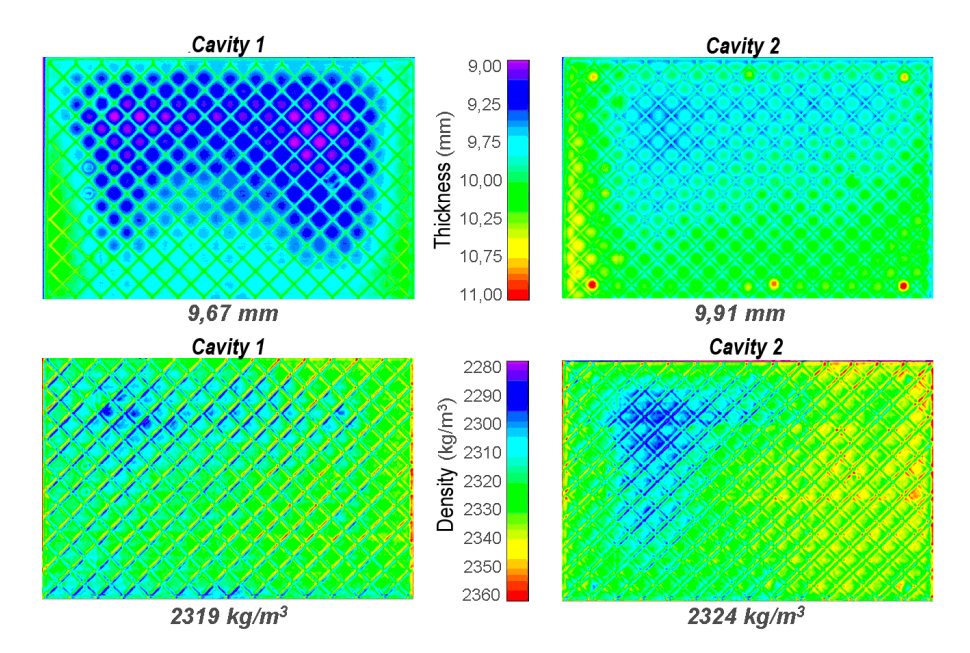


Figure 10. Thickness distributions (top) and bulk density distributions (bottom) of two fired porcelain tiles.

When tile 2 was pressed, however, this compensation did not occur (the round shape of the thickness distributions in the regions located between the ribs indicates lack of oil in the isostatic punch, which allowed the rubber lining on the punch to deform), thus producing a tile with a very similar average bulk density to that of the tile obtained in cavity 1, but with a higher average thickness and a bulk density distribution with average maximum differences of about 50 kg/m³.

The non-destructive character of the method enabled the same tiles to be analysed after they had been subjected to an industrial firing cycle with a peak temperature of 1200°C and the influence of the sintering process on end-product properties thus to be evaluated. The thickness and fired bulk density distributions of the two studied tiles are depicted in figure 10. The fired density distributions show that the heterogeneities produced in pressing in tile 2 remained present after the firing, albeit to a lesser extent, as a result of the minor influence of dry density on fired density exhibited by porcelain tile compositions at high firing temperatures [9].

The example provided demonstrates the usefulness of the X-ray absorption method in identifying, among other matters, the origin of manufacturing defects relating to lack of dimensional stability in the end product. Indeed, the possibility of characterising the same tiles, before and after firing, enables it to be established whether a given defect is due to an inappropriate pressing operation or, in contrast, is produced by bad kiln regulation.



4. **CONCLUSIONS**

The following conclusions may be drawn from the study:

An apparatus has been designed and built, based on the X-ray absorption technique, which allows bulk density distributions to be precisely and non-destructively measured in large-sized ceramic tiles.

The apparatus provides complementary information on thickness and mass distributions, which is of great interest for the optimisation of the ceramic tile forming process.

It has been verified that the apparatus enables defects relating to heterogeneous bulk density distribution caused by an inappropriate pressing operation to be detected.

The non-destructive character of the apparatus allows fired tiles, which had previously been characterised in an unfired state, to be examined with a view to evaluating the effect of the firing and pressing stages on end-product properties.

ACKNOWLEDGEMENTS

The authors of this paper wish to thank IMPIVA for its financial support in conducting the study, through the programme for the support of R&D in technology centres of the Impiva network.

REFERENCES

- [1] AMORÓS, J. L. Pastas cerámicas para pavimentos de monococción: Influencia de las variables de prensado sobre las propiedades de la pieza en crudo y sobre su comportamiento durante el prensado y la cocción. Valencia: Universidad. 1987, p.61 [Tesis doctoral].
- [2] AMORÓS, J. L. et al. Técnicas experimentales del control de la compactación de pavimentos y revestimientos cerámicos. Técnica Cerámica, 116, 1234-1246, 1983.
- [3] ENRIQUE, J. E. et al. Alternativas al método de inmersión en mercurio para la determinación de la densidad aparente de baldosas cerámicas. Técnica Cerámica, 250. 18-27, 1997.
- [4] AMORÓS, J. L. et al. Medida no destructiva de la densidad aparente de piezas en crudo mediante absorción de rayos X. En: Qualicer 2006. IX Congreso Mundial de la Calidad del Azulejo y del Pavimento Cerámico. Castellón: Cámara oficial de Comercio, Industria y Navegación, 2006.



- [5] CANTAVELLA, V. et al. Uso de la técnica de ultrasonidos para medir la densidad aparente de baldosas en crudo y optimizar el proceso de prensado. Cerámica Información, 345. 77-84, 2007.
- [6] Método y aparato no destructivo para la medida de la densidad en baldosas cerámicas. Amorós, J. L.; Cantavella, V.; Llorens, D.; Feliu, C. Patente PCT/ES2005/000397.
- [7] BERTIN, E. P. Principles and practice of X-Ray spectrometric analysis. New York: Plenum Press 1984, pp. 51-55.
- [8] PHILLIPS, D. H. et al. Measuring physical density with X-ray computed tomography. NDT & E Internacional, Vol. 30, No. 6, pp. 339-350, 1997.
- [9] BAGÁN, V. Efecto de las condiciones de operación en las diferentes etapas del proceso sobre las propiedades y características de pavimento de muy baja porosidad. Valencia: Universidad. 1991, p.191 [Tesis doctoral].